Austenite in Advanced High Strength Steels

Subjects: Materials Science, Characterization & Testing

Contributor: Binbin He

Advanced high strength steels (AHSS) are developed to reduce vehicle weight without sacrificing passenger safety. The newly developed AHSS frequently incorporates the austenite as the intrinsic component with large amount and good stability, which is realized by carefully designed alloying elements and thermo-mechanical processing.

mechanical behavior martensite deformation twins

1. Introduction

The advanced high strength steels (AHSS) are developed to overcome the trade-off between the reduction of vehicle weight and the increase of passenger crashworthiness [1]. The ultrahigh strength of AHSS allows the design of thinner structural components and lighter automobiles while protecting the passengers from the anti-intrusion events [2]. The good ductility of AHSS ensures the large energy absorption during the central collision, the easy fabrication of complex structural components, and the observed deformation before the sudden failure [2].

2. Austenite in AHSS

The austenite grains in the 3rd generation of AHSS demonstrate the different microstructural features which are determined by the presence of varied defects, including the point defects (interstitial/substitutional atoms), line defects (dislocations), and area defects (stacking faults/twins/boundary) [3]. Among these defects, the grain boundary is the most important one as it determines the domain, size, and morphology of the austenitic single crystal for the storage of other defects. In general, the defects in austenite grains are derived from prior phase transformation during the thermo-mechanical processing. The austenite grains in Q&P steel demonstrates blocky and film-like morphologies (**Figure 1**a) [4], which is related to the extent of the martensitic transformation. In particular, the extensive martensitic transformation leads to the severe partition of prior austenite grain into film-like retained austenite while the moderate martensitic transformation results in the co-existence of blocky and film-like residual austenite. The above observation is also applicable for the austenite grains in the CFB steel considering the displacive nature of bainitic transformation (**Figure 1**b) [5]. The number of defects in the retained austenite grains including dislocations, stacking faults, and deformation twins depends on the extent of phase transformation. The austenite grains retained after displacive shear transformation (martensitic/bainitic transformation) are deformed to accommodate the transformation strain of the adjacent transformed products [6]. The defect density in austenite grains is heterogeneous owing to the localized deformation process, demonstrating increased defect density with the decrease of distance to the interface of austenite and product phase [7]. Since the blocky austenite

grains are subjected to less extensive martensitic transformation, they are expected to have lower amounts of internal defects than that of filmy-like counterparts. The retained austenite grains in medium Mn steel are generally obtained by reverse transformation from either quenched or deformed martensite, generating the lamellar or granular austenite grains, respectively (**Figure 1**c) [8]. In addition, the morphology of austenite grains in medium Mn steel also depends on the extent of reverse transformation. The reverse transformation from ferritic phase to austenite with different durations results in austenite grains with either lamellar or granular morphology [9]. Although the mechanism of reverse transformation deviates from the displacive shear transformation, the lamellar austenite grains in medium Mn steel exhibit higher dislocation density than the granular counterpart, which can be rationalized from the concurrence of dislocations recovery or recrystallization with prolonged duration [10].

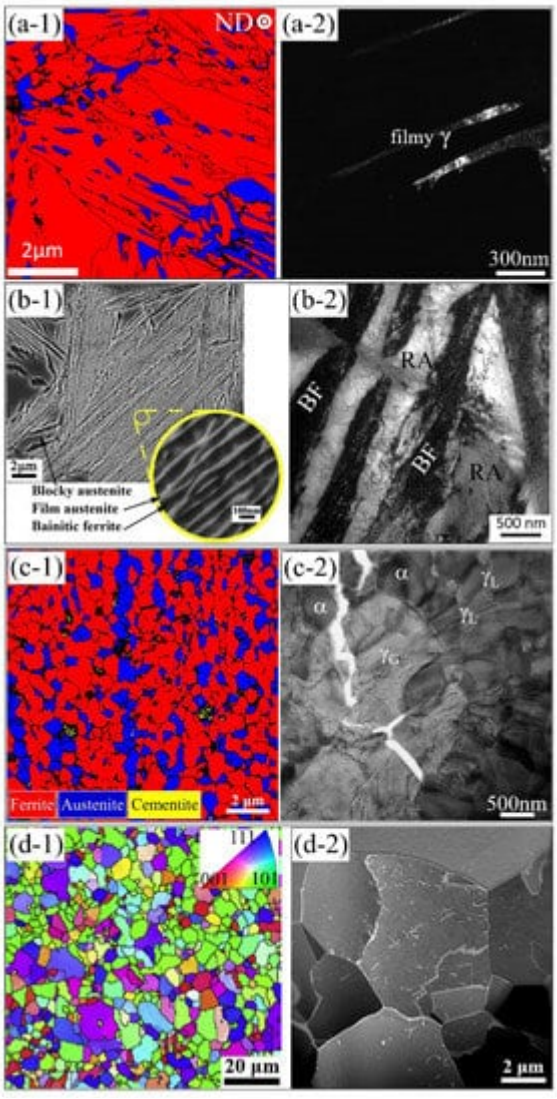

Figure 1. Microstructure of different AHSS containing the metastable austenite grains, including the (**a**) Q&P steel [11], Reprinted with permission from ref. [11]. Copyright 2018, Elsevier. (**b**) CFB steel [12][13], Reprinted with permission from ref. [12][13]. Copyright 2015, 2017, Elsevier. (**c**) medium Mn steel [14][15], Reprinted with permission from ref. [14][15]. Copyright 2019, 2021, Elsevier. and (**d**) TWIP steel [16][17]. Reprinted with permission from ref. [16][17],. Copyright 2015, 2016, Elsevier. (**a-1**) and (**c-1**) are EBSD phase map; (**b-1**) is SEM image; (**d-1**) is EBSD

orientation map; (**a-2**) to (**d-2**) are TEM images. Red color and blue color in (**a-1**) represent the martensite and austenite, respectively. ND: normal direction. γ_G: granular austenite; γ_L: lamellar austenite; α: ferrite.

The phase transformation is frequently associated with element partitioning between the ferritic and austenitic phases during the thermo-mechanical processing of 3rd generation of AHSS. Owing to the relatively low partitioning temperature in Q&P steel and the low bainitic transformation temperature in CFB steel, only the C partitioning from the ferritic phase to the austenite phase is observed while the Mn partitioning is negligible [18][19]. In contrast, the intercritical annealing temperature is sufficiently high to allow both Mn and C partitioning in the medium Mn steel [20][21][22]. The element enrichment (C, Mn), dislocations, and ultrafine grain size are all contributing to the stabilization of austenite grains at ambient temperature [20][21][22]. Therefore, the austenite grains in the 3rd generation of AHSS demonstrate unique microstructural features as compared to the ferritic counterpart, including the different morphologies, higher interstitial/substitutional elements, and heterogeneous distribution of dislocations.

Different from the complex phase transformation and element partitioning involved in the processing of the 3rd generation of AHSS, only typical recrystallization, and dislocation recovery is necessary for the fabrication of 2nd generation of AHSS (i.e., TWIP steel as shown in **Figure 1**d) [23][24]. The grain size of the austenite can be tuned by controlling the austenitization temperature and durations. The heterogeneous grained structure with twinned and untwined austenitic phase can be generated in TWIP steel (Fe-22Mn-0.6C in wt.%) by employing the severe plastic deformation and subsequent controlled annealing at 600 °C with partial recrystallization [25]. The prolonged aging treatment of deformed TWIP steel at 400 °C for 336 h may lead to the decomposition of austenite into pearlite at the highly deformed regions with intensive cementite precipitations [25]. The nanotwined steel can be produced by cold deformation of the TWIP steel system (Fe-17.59Mn-0.75C-1.7Al-0.52Si in wt.%) with the generation of deformation twins and dislocations, followed by dislocation recovery process to regain the strain hardening capacity [26]. The phase transformation is absent during the cold deformation of TWIP steel and the cementite precipitation can be avoided by reducing the duration of recovery annealing such as 500 °C for 15 min [26].

References

1. Kuziak, R.; Kawalla, R.; Waengler, S. Advanced high strength steels for automotive industry. Arch. Civ. Mech. Eng. 2008, 8, 103–117.
2. Bouaziz, O.; Zurob, H.; Huang, M. Driving Force and Logic of Development of Advanced High Strength Steels for Automotive Applications. Steel Res. Int. 2013, 84, 937–947.
3. He, B. On the Factors Governing Austenite Stability: Intrinsic versus Extrinsic. Materials 2020, 13, 3440.
4. Xiong, X.C.; Chen, B.; Huang, M.X.; Wang, J.F.; Wang, L. The effect of morphology on the stability of retained austenite in a quenched and partitioned steel. Scripta Mater. 2013, 68, 321–

324.

5. Bhadeshia, H.; Edmonds, D. The mechanism of bainite formation in steels. Acta Metall. 1980, 28, 1265–1273.
6. Greenwood, G.W.; Johnson, R.H. The Deformation of Metals Under Small Stresses During Phase Transformations. Proc. R. Soc. Lond. A 1965, 283, 403–422.
7. He, B.B.; Wang, M.; Huang, M.X. Improving Tensile Properties of Room-Temperature Quenching and Partitioning Steel by Dislocation Engineering. Metall. Mater. Trans. A 2019, 50, 4021–4026.
8. Han, J.; Lee, S.-J.; Jung, J.-G.; Lee, Y.-K. The effects of the initial martensite microstructure on the microstructure and tensile properties of intercritically annealed Fe–9Mn–0.05 C steel. Acta Mater. 2014, 78, 369–377.
9. Han, Q.; Zhang, Y.; Wang, L. Effect of annealing time on microstructural evolution and deformation characteristics in 10Mn1. 5Al TRIP steel. Metall. Mater. Trans. A 2015, 46, 1917–1926.
10. Chbihi, A.; Barbier, D.; Germain, L.; Hazotte, A.; Gouné, M. Interactions between ferrite recrystallization and austenite formation in high-strength steels. J. Mater. Sci. 2014, 49, 3608–3621.
11. Liu, L.; He, B.; Cheng, G.; Yen, H.; Huang, M. Optimum properties of quenching and partitioning steels achieved by balancing fraction and stability of retained austenite. Scripta Mater. 2018, 150, 1–6.
12. Gong, W.; Tomota, Y.; Harjo, S.; Su, Y.H.; Aizawa, K. Effect of prior martensite on bainite transformation in nanobainite steel. Acta Mater. 2015, 85, 243–249.
13. Beladi, H.; Tari, V.; Timokhina, I.B.; Cizek, P.; Rohrer, G.S.; Rollett, A.D.; Hodgson, P.D. On the crystallographic characteristics of nanobainitic steel. Acta Mater. 2017, 127, 426–437.
14. Wang, X.; He, B.; Liu, C.; Jiang, C.; Huang, M. Extraordinary Lüders-strain-rate in medium Mn steels. Materialia 2019, 6, 100288.
15. Liang, Z.Y.; Cao, Z.H.; Lu, J.; Huang, M.X.; Tasan, C.C. Influence of co-existing medium Mn and dual phase steel microstructures on ductility and Lüders band formation. Acta Mater. 2021, 117418.
16. Liang, Z.; Wang, X.; Huang, W.; Huang, M. Strain rate sensitivity and evolution of dislocations and twins in a twinning-induced plasticity steel. Acta Mater. 2015, 88, 170–179.
17. Liang, Z.Y.; Li, Y.Z.; Huang, M.X. The respective hardening contributions of dislocations and twins to the flow stress of a twinning-induced plasticity steel. Scripta Mater. 2016, 112, 28–31.

18. Speer, J.; Matlock, D.; De Cooman, B.; Schroth, J. Carbon partitioning into austenite after martensite transformation. Acta. Mater. 2003, 51, 2611–2622.
19. Lawrynowicz, Z. Carbon partitioning during bainite transformation in low alloy steels. Mater. Sci. Technol. 2002, 18, 1322–1324.
20. Lee, S.; Lee, S.J.; De Cooman, B.C. Austenite stability of ultrafine-grained transformation-induced plasticity steel with Mn partitioning. Scripta. Mater. 2011, 65, 225–228.
21. Luo, H. Comments on “Austenite stability of ultrafine-grained transformation-induced plasticity steel with Mn partitioning” by S. Lee, S.J. Lee and B.C. De Cooman, Scripta Materialia 65 (2011) 225–228. Scripta Mater. 2012, 66, 829–831.
22. Lee, S.; Lee, S.-J.; De Cooman, B.C. Reply to comments on “Austenite stability of ultrafine-grained transformation-induced plasticity steel with Mn partitioning”. Scripta Mater. 2012, 66, 832–833.
23. Bracke, L.; Verbeken, K.; Kestens, L.; Penning, J. Microstructure and texture evolution during cold rolling and annealing of a high Mn TWIP steel. Acta Mater. 2009, 57, 1512–1524.
24. Haase, C.; Ingendahl, T.; Güvenç, O.; Bambach, M.; Bleck, W.; Molodov, D.A.; Barrales-Mora, L.A. On the applicability of recovery-annealed twinning-induced plasticity steels: Potential and limitations. Mater. Sci. Eng. A 2016, 649, 74–84.
25. Xiong, T.; Zheng, S.; Zhou, Y.; Pang, J.; Jin, Q.; Ge, H.; Zheng, X.; Yang, L.; Beyerlein, I.; Ma, X. Enhancing strength and thermal stability of TWIP steels with a heterogeneous structure. Mater. Sci. Eng. A 2018, 720, 231–237.
26. Zhou, P.; Liang, Z.Y.; Liu, R.D.; Huang, M.X. Evolution of dislocations and twins in a strong and ductile nanotwinned steel. Acta Mater. 2016, 111, 96–107.